Master's Thesis

Numerical Study of Hydrogen Inhibition of Char

Author:
Joanna Lazar

Supervisor:
Nils Erland L. Haugen

Supervisor:
Andrzej Szlek

Norwegian University of Science and Technology
Faculty of Engineering Science and Technology
Department of Energy and Process Engineering

Silesian University of Technology
Faculty of Engergy and Environmental Engineering
Department of Environmental Engineering

Trondheim, July 2015

Abstract

It has been known for a long time that hydrogen in the gas phase tend to inhibit gasification of char at low and intermediate temperatures. At higher temperatures, however, there are indications that hydrogen may speed up gasification. The mechanisms behind this effects are currently not understood. In this work, a newly developed detailed chemical kinetics model for char has been used in order to study the mechanisms behind the hydrogen inhibition and speed-up of char gasification. For conditions assumed in this work, the hydrogen inhibition is found for $T < 2000K$, while for $T > 2000K$ the hydrogen in the gas phase speeds up the char conversion. By studying the species reaction rates together with the individual rate of every single reaction, the reasons for hydrogen influence on the char gasification are explained in this paper.

Acknowledgments

This work forms part of the CAMPS project supported by the Research Council of Norway (215707). The work has additionally been produced with support from the BIGCCS Centre, performed under the Norwegian Research Program Centres for Environment-Friendly Energy Research (FME). The author acknowledges the following partners for their contributions: Aker Solutions, ConocoPhillips, Gassco, Shell, Statoil, TOTAL, GDF SUEZ and the Research Council of Norway (193816/S60).

The research leading to these results has been received funding from the Polish-Norwegian Research Programme operated by the National Centre for Research and Development under the Norwegian Financial Mechanism 2009-2014 in the frame of Project Contract No Pol-Nor/232738/101/2014.

The author also acknowledges the SINTEF Energy Research for their support.

Contents

List of Figures

List of Tables

1. Introduction

Gasification is one of the clean energy technologies. It is a process of the converting any material containing carbon, such as coal, biomass and others, into more useful gaseous form (synthesis gas, syngas). Syngas can be used for electricity and heat production in a high-efficiency devices, such as internal combustion engines and gas turbines. Currently, the gasification is commonly used to generate power in Integrated Gasification Combined Cycle (IGCC), as well as to produce chemicals and transportation fuels. In the gasifier, a several different processes of the conversion of the carbonaceous material occur, such as devolatilization (which consists in release of volatiles and production of char due to the heating up and drying a fuel particle), and the following gasification. A limited amount of oxygen, just enough to provide the heat for gasification, is introduced into the gasifier. The gasification process is slower than the devolatilization process. Simplifying, it involves the production of carbon monoxide and hydrogen as a result of reactions of the char with carbon dioxide and steam.

In the current work, a newly developed detailed chemical kinetics model for char has been used in order to study the mechanism behind the hydrogen inhibition of char gasification at low and intermediate temperatures. It has been also investigated the effect of speed-up gasification process at higher temperatures. In order to check the impact of hydrogen on char gasification, the results of conversion simulations assuming two of the reactions, with hydrogen molecule on the reactant side, to be active or not are compared. Deactivating a reaction means turning it off by temporarily setting its pre-exponential factors to zero.

In this work, the focus is on the gasification of the coal char, however it is predicted, that the results would be similar for a research based on the gasification of the other fuels such as biomass.

The char conversion process is influenced by the chemical reaction rates and the rates of the transport of the gas phase to the particle outer surface and through its pores. The char conversion can proceed in one of three particular regimes. Depending of the two following, chemistry or mass transport, is dominating in the process of the conversion. For small particle size ($< 150\mu$m) the temperature has a great impact, what has been described previously in the work of Mitchell *et al.* [1]. At low temperatures ($<\sim$ 900 K), the conversion is proceed in the zone I conversion regime, where the chemical reaction rates are considerably slower than the mass transport rates. The gas penetrates the char particle and the particle reacts throughout its volume. The size of the particle almost does not change and its apparent density decreases (proportionally with decreasing particle mass). In the zone I conversion regime the rates of char conversion are limited by the rates of the chemical reactions. At high temperatures ($>\sim$ 1800 K), the conversion is proceed in zone III conversion regime, where the mass transport rates are slow

in comparison to the chemical reaction rates. The gas does not penetrate the particle,chemical reactions take place mainly at particle periphery. The size of the char particle decreases and its apparent density relatively does not vary. In zone III conversion regime the rates of char conversion are limited by the rates that gas diffuses to the particle surface. Between zone I and zone III is the zone II conversion regime ($>\sim$ 900 K and $<\sim$ 1800 K). During gasification in the zone II conversion regime the size and apparent density of the char particle decrease with mass loss. In this regime the rates of char conversion are limited by both the chemical reaction rates and the mass transport rates. This regime is the most difficult to model, considering that penetration of the particle by gas might not be complete. The solution employed in this work is the modeling strategy developed by Thiele [2]. In mentioned approach an effectiveness factor is used to solve the issue of particle incomplete penetration.

In this paper, the calculations in the model are made on a single particle, the one of many in the particle cloud. It is assumed that all other particles behave in the same way as the considered one.

In the current work, the model assumes that during exposure of the particle to the hot reactive gases (O_2 and CO_2), the mass, apparent density and size of the particle change with time. Between the particle and the gas phase occur detailed, finite rate heterogeneous reactions. The gas phase species are adsorbed on the internal and external surface of the particle and react with the carbonaceous part of the particle. The conversion of the char proceeds. Desorbed species may then react with the other gas phase species due to detailed, finite rate homogeneous reactions. Moreover it is predicted that between the particle and gas phase the heat is transferred due to convection and conduction. The model also takes into account the radiation exchange between the particles in the cloud, as well as the radiation between a particle and the wall of the gasifier.

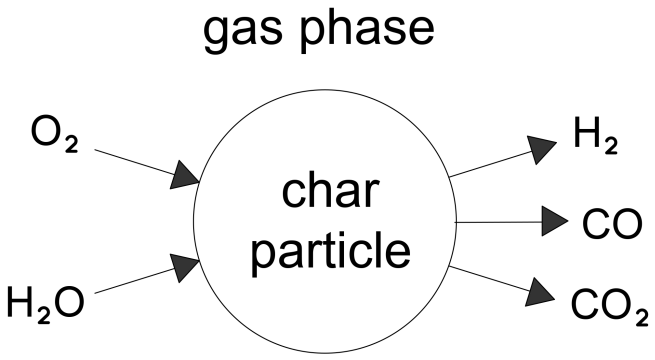

Figure 1: Simplified model of char gasification (created in AutoCAD [3]).

In the following sections, the essentials of the numerical model used to simulate the char gasification, as well as the results of the studies on hydrogen impact of char are described. In the "Results" section, the figures showing the outcomes of the char conversion simulations are presented. It can be seen that the results are very similar for cases A and C as well as for cases B and D, such as lines representing results are exactly on top of each other. It can be also noted that lines in the plots are not smooth. There are atypical peaks for cases A and C for t=0,12 s and t=0,31 s. It may be noticed, that these two points could be simply linked by the line following predicted path. The reason of the peaks occurrence is not exactly understood. However, it seems to not have any consequential effect on the general results. It should be noticed, that the mechanism employed in this work has been developed to study process of char gasification at low temperatures. Indeed, it has been observed that for the simulations at very high temperature, mechanism does not work correctly. In the following section, "Impact of the temperature inside the reactor" the results for the simulation of char gasification in wide temperature range are presented. In the plots prepared for the conversion at very high temperature an anomalous peaks occur, that can not be explained at this stage of the research. It should be taken into account in the future works that the mechanism is valid just for temperature, which for, it has been originally designed.

2. Model description

In this section the essentials of the numerical model used to simulate the char gasification are described. For more details on the model, the reader is referred to Haugen, Mitchell and Tilghman (2015) [4].

In the following, particles are assumed to be spherical and uniform in composition and morphology, while the ash is uniformly distributed throughout the particle volume. In addition, ash in the char can not react or be evaporated, and there is no exchange of mineral matter between the particle and the gas phase.

Let V be considered as the volume, containing a uniform gas-particle mixture. The number of embedded char particles in the cloud, N_p, is constant. The surface S, which is impermeable (there is no mass flux across S) and flexible (the gas pressure is kept constant), encloses the volume V. The total mass m enclosed by surface S is then constant and can be written as

$$m = m_p N_p + m_g, \tag{1}$$

where m_p is the mass of a single particle and m_g is the mass of the gas. The gas density is given by

$$\rho_g = \frac{m_g}{V - N_p V_p}, \tag{2}$$

where V_p is the volume of a single particle. The particle number density is given by

$$n_p = \frac{N_p}{V}. \tag{3}$$

The exchange of matter between the particles and the ambient gas is caused by reactions between the gas and the solid phase. The species production rate can be symbolized by $\omega_{pg,i}$ for the particle-to-gas reactions and $\omega_{gg,i}$ for the gas-to-gas reactions. These two terms determine the change of the mass fractions of the species i in the gas phase.

The heterogeneous reaction mechanism, based on the work of Haynes (2001) [5], is shown in Table 1. The mechanism is described by Tilghman and Mitchell [6]. In the reaction scheme, the adsorbed species $C(H)$, $C(O)$, $C(CO)$, $C(OH)$ represent a hydrogen atom, oxygen atom, carbon monoxide and OH group adsorbed on a carbon site, respectively, while $C_2(O_2)$ represent two adjacent carbon sites that has adsorbed one oxygen atom each. The bulk carbon site, C_b, is a carbon atom bonded to the four other carbon atoms. As a result of chemical reactions, the bulk carbon site can become a free carbon site. The free carbon site, C_f, is a carbon atom that is available for adsorption of gas phase species. Due to the particle-to-gas reactions, the oxygen, carbon and hydrogen compounds desorb from the carbonaceous matrix and leave the particle surface. As a result of this process, an underlying carbon atom becomes the free carbon site.

Table 1: The heterogeneous reaction mechanism.

Nr.	Reaction			A_k	E_k	σ_k
R1	$2C_f + H_2O$	$\leftrightarrow$	$C(OH) + C(H)$	7.3×10^7	106	0
R2	$C(OH) + C_f$	$\leftrightarrow$	$C(O) + C(H)$	1.5×10^{12}	150	0
R3	$C(H) + C(H)$	$\leftrightarrow$	$H_2 + 2C_f$	1.0×10^{12}	100	0
R4	$C(O) + C_b$	$\rightarrow$	$CO + C_f$	1.0×10^{13}	353	28
R5	$C(OH) + C_b$	$\leftrightarrow$	$HCO + C_f$	1.0×10^{13}	393	28
R6	$C_b + C_f + C(H) + H_2O$	$\leftrightarrow$	$CH_3 + C(O) + C_f$	1.0×10^{13}	300	0
R7	$C_b + C_f + C(H) + H_2$	$\leftrightarrow$	$CH_3 + 2C_f$	1.0×10^{13}	300	0
R8	$C_f + C(H) + CO$	$\rightarrow$	$HCO + 2C_f$	1.0×10^{13}	300	0
R9	$C(H) + C(H)$	$\rightarrow$	$CH_2 + C_f$	3.0×10^{11}	426	0
R10	$CO_2 + C_f$	$\leftrightarrow$	$C(O) + CO$	8.6×10^4	188	0
R11	$C_b + CO_2 + C(O)$	$\rightarrow$	$2CO + C_f$	3.26×10^{12}	367	0
R12	$C(CO)$	$\leftrightarrow$	$CO + C_f$	1.0×10^{13}	455	53
R13	$CO + C(CO)$	$\rightarrow$	$CO_2 + 2C_f$	3.36×10^6	266	0
R14	$2C_f + O_2$	$\rightarrow$	$C(O) + CO$	7.0×10^{10}	150	0
R15	$2C_f + O_2$	$\rightarrow$	$C_2(O_2)$	3.0×10^8	103	0
R16	$C_f + C_b + C(O) + O_2$	$\rightarrow$	$CO_2 + C(O) + C_f$	1.5×10^7	78	0
R17	$C_f + C_b + C(O) + O_2$	$\rightarrow$	$CO + 2C(O)$	2.1×10^7	103	0
R18	$C_b + C_2(O_2)$	$\rightarrow$	$CO_2 + 2C_f$	1.0×10^{13}	304	33

* Arrhenius parameters shown in the table were obtained for Wyodak coal [7].

In this paper, the focus is on two of the mechanism reactions, R3b and R7f, with the hydrogen molecule on the reactant side. Studying the hydrogen inhibition on char gasification, the results of conversion simulations assuming these two reactions to be active or not are compared.

Let k define a reaction from the set of N_r =18 heterogeneous reactions listed in Table 1 and let i define a reacting species, gas phase species or adsorbed species. Adsorption and desorption due to reaction k is given then by the generalized equation

$$\sum_{i=1}^{N_{s,gas}+N_{s,ads}} \nu_{i,k}\alpha_i \leftrightarrow \sum_{i=1}^{N_{s,gas}+N_{s,ads}} \nu'_{i,k}\alpha_i, \tag{4}$$

where $N_{s,gas}$ is the number of gas phase species and $N_{s,ads}$ is the number of adsorbed species. Species i is symbolized by α_i. Stoichiometric coefficients are represented by $\nu_{i,k}$ for species on the reactant side and by $\nu'_{i,k}$ for species on the product side of reaction k.

2.1. Governing gas phase equations

The gas phase is defined by three governing equations describing the evolution of mass, species and temperature in the gas phase. The first equation describes the evolution of the gas phase mass, m_g:

$$\frac{dm_g}{dt} = \frac{m_g}{\rho_g} \sum_{i=1}^{N_{s,gas}} \omega_{pg,i} M_i, \tag{5}$$

where ρ_g is the mass density of the gas phase and M_i is the molar mass of species i. The second equation describes the total mass fraction of species i in the gas phase:

$$\rho_g \frac{dY_i}{dt} + Y_i \sum_{k=1}^{N_{s,gas}} \omega_{pg,k} M_k = (\omega_{gg,i} + \omega_{pg,i}) M_i, \tag{6}$$

where Y_i is the mass fraction of species i. The third equation is the energy equation:

$$\rho_g c_{p,g} \frac{dT_g}{dt} + \sum_{i=1}^{N_{s,gas}} h_i (\omega_{gg,i} + \omega_{pg,i}) M_i = n_p (Q_h + Q_c), \tag{7}$$

where $c_{p,g}$ is the heat capacity of the gas mixture at constant pressure, T_g is the temperature of the gas, h_i is the enthalpy of species i, Q_h is the energy transfer from the solid phase to the gas phase due to heterogeneous reactions and Q_c is the heat transfer from the particle to the gas mixture due to convection and conduction.

2.2. Governing solid phase equations

In this subsection, the governing equations describing mass transport and chemical reactions in the solid phase (the char) are presented.

2.2.1. Particle mass

The evolution of the carbonaceous part of the char particle mass is described by

$$\frac{dm_c}{dt} = \dot{m}_c = -S_t M_c R_{reac,c}, \tag{8}$$

where M_c is the molar mass of carbon, $R_{reac,c}$ is the molar reaction rate of carbon and S_t is the total surface area of the carbonaceous part of the particle, given by

$$S_t = S_{gc} m_c, \tag{9}$$

where S_{gc} is the specific surface area of the carbonaceous part of the char particle. Based on Eq. (8) and Eq. (9) the equation for the carbonaceous fraction of the char particle mass may be rewritten as

$$\frac{1}{m_c}\frac{dm_c}{dt} = \frac{\dot{m}_c}{m_c} = -S_{gc}R_{reac,c}M_c. \tag{10}$$

The production rate of carbon per total particle surface area for reaction k is given by

$$R_{c,k} = M_c \sum_{i=1}^{N_{s,gas}} R_{reac,k}(\nu'_{i,k} - \nu_{i,k})a_{c,i}, \tag{11}$$

where $R_{reac,k}$ is molar reaction rate for reaction k and $a_{c,i}$ is the number of carbon atoms in species i. For reaction k the carbon consumption rate can be defined as

$$\dot{m}_{c,k} = -S_t R_{c,k}. \tag{12}$$

The evolution of the carbonaceous part of the particle volume specific surface area for conversion in the zone I conversion regime is given by

$$S_{vc} = S_{vc,0}(1-x)\sqrt{1-\psi\ln(1-x)}, \tag{13}$$

where ψ is the structural parameter and x is the conversion of the carbonaceous part of the particle. Subscript 0 symbolizes the initial conditions in the char conversion process. Since variations of the apparent density of the carbonaceous part of the particle, ρ_c, is proportional to variations of the mass of the carbonaceous part of the particle, m_c, in the zone I conversion regime, it is true that

$$\frac{m_c}{m_{c,0}} = \frac{\rho_c}{\rho_{c,0}} = 1 - x, \tag{14}$$

such that Eq. (13) can be rewritten as

$$S_{vc} = S_{vc,0}\frac{\rho_c}{\rho_{c,0}}\sqrt{1-\psi\ln(\frac{\rho_c}{\rho_{c,0}})}. \tag{15}$$

Based on the relationship

$$S_{gc} = \frac{S_{vc}}{\rho_c}, \tag{16}$$

Eq. (15) can be modified to express the evolution of the specific surface area of the carbonaceous part of the particle during the char conversion as

$$S_{gc} = S_{gc,0}\sqrt{1-\psi\ln(\frac{\rho_c}{\rho_{c,0}})}. \tag{17}$$

Since in the zone III conversion regime the particle apparent density is constant, the particle mass specific area should also remain constant. According to the statement above, Eq. (17) is found to be correct for gasification of char both in zone I and zone III conversion regimes. The model is assumed to be flexible, such that the char conversion can proceed in any of the three regimes. Since it is valid both for zone I and III, it seems sensible to expect Eq. (17) to be valid also for gasification in zone II conversion regime.

The mass of the particle, including ash, is given by

$$m_p = m_c + m_a = m_c + X_a m_{p,0} = m_c + \frac{X_a m_{c,0}}{1 - X_a}, \tag{18}$$

where m_a and X_a are the mass and initial mass fraction of the mineral matter in the particle, respectively.

2.2.2. Particle temperature

The temperature of char particle is determinated by

$$\frac{dT_p}{dt} = \frac{1}{m_p c_{p,p}} \left(Q_{reac} - Q_c + Q_{rad} \right), \tag{19}$$

where T_p is the particle temperature and $c_{p,p}$ is the specific heat capacity of the particle. The heating due to heterogeneous reaction, Q_{reac}, depends on the total surface area of the carbonaceous part of the particle, S_t, the molar reaction rate, $RR_{reac,k}$, and the molar heat of reaction, $q_{reac,k}$ for all reactions k in mechanism. Heat of reaction, $q_{reac,k}$ is the function of the enthalpy of formation of species i, h_i, evaluated at the temperature of the particle. The heat transfer from the char particle to the gas phase via convection and conduction is represented by Q_c. The heating due to radiation, Q_{rad} from the char particle to the reactor wall is defined by Stefan-Boltzmanns equation. The radiation between the particles and the gas phase is not taken into account. The inter-particle radiation is considered, though. The position of the particle in the particle cloud becomes important, so the heat transfer due to radiation, Q_{rad}, depends also on the particle number density, the reactor enclosure radius and the absorption coefficient of the cloud via absorption of radiant energy by the particles.

2.2.3. Adsorbed species

The species adsorbed on the particle internal and external surface is symbolized by j. The number of moles of adsorbed species j is given by

$$N_j = C_{s,j} S_t, \tag{20}$$

where $C_{s,j}$ is the concentration of adsorbed species j on the surface of the char particle. The rate of change in the site fraction of species j is given by

$$\frac{d\Theta_j}{dt} = \frac{R_{spec,j}}{\xi_n} + AR_{reac,c}\Theta_j, \tag{21}$$

where Θ_j is the adsorbed species site fraction, that is the ratio between the concentration of adsorbed species, $C_{s,j}$, and the total surface concentration of both free and occupied carbon sites, ξ_n. The molar rate of adsorbed species production is symbolized by $R_{spec,j}$. The term A appearing in Eq. (21) can be expressed as

$$A = (1 - \frac{S_{t,0}^2 \psi (1-x)^2}{2S_t^2}) S_{gc} M_c. \tag{22}$$

The free carbon sites fraction is given by

$$\Theta_{cf} = 1 - \sum_{i \neq cf} \Theta_i, \tag{23}$$

where Θ_i is the site fraction of species i.

2.3. Species concentrations at the particle surface

The relationship between the flux of gas phase species i through the boundary layer to the external particle surface and net production of species i via particle-to-gas reactions, in steady state, is given by

$$\dot{n}_i - X_{i,s}\dot{n}_{total} = -k_{im}(X_{i,\infty} - X_{i,s}), \tag{24}$$

where $X_{i,\infty}$ is the mole fraction of species i in the ambient gas phase and $X_{i,s}$ is the mole fraction of species i at the particle surface. The species mass transfer coefficient is represented by k_{im}. The molar flux of all species i, $\dot{n}_{total}$ and each species i, $\dot{n}_i$ are expressed, respectively, as

$$\dot{n}_{total} = \sum_{i=1}^{N_{s,gas}} \dot{n}_i \tag{25}$$

and

$$\dot{n}_i = \sum_{k=1}^{N_r} \dot{n}_{i,k}. \tag{26}$$

In Eq. (26) $\dot{n}_{i,k}$ is the molar flux of species i due to reaction k and is defined as

$$\dot{n}_{i,k} = (\nu'_{i,k} - \nu_{i,k}) R_{reac,k} \frac{S_t}{A_p}, \tag{27}$$

where A_p is the external surface of the particle. The species molar production rate from a single particle is expressed as $\dot{n}_i A_p$. The species molar production rate from all the particles in the cloud is then given by

$$\omega_{pg,i} = \dot{n}_i A_p n_p. \tag{28}$$

When the distance between the particles in the cloud is significantly larger than the radius of a particle, the mass transfer coefficient of species i is expressed by the relationship

$$k_{im} = \frac{C_g D_{im}}{r_p}, \tag{29}$$

where r_p is the particle radius, D_{im} is the molecular bulk diffusivity of species i and

$$C_g = \frac{\rho}{\overline{M}} = \frac{P}{RT_f} \tag{30}$$

is the concentration of gas close to the particle surface. In the equation above ρ, $\overline{M}$, P and R are the density, average molar mass, pressure and universal constant of the gas, respectively. The temperature of the gaseous shell around the particle is given by

$$T_f = T_p + \frac{1}{3}(T_g - T_p). \tag{31}$$

2.4. Surface reactions

The molar rate of reaction k is given by

$$R_{reac,k} = k_k \prod_{i=1}^{N_{s,gas}+N_{s,ads}} C_i^{\nu_{i,k}}, \tag{32}$$

where k_k is the rate coefficient of reaction k. The concentration of species i is represented by C_i. Symbol $\nu_{i,k}$ specifies that just species on the reactant side of reaction k are taken into account in Eq. (32). The molar production rate of species i, via all reactions in mechanism, is given by

$$R_{spec,i} = \sum_{k=1}^{N_r} (\nu'_{i,k} - \nu_{i,k}) R_{reac,k}. \tag{33}$$

The rate coefficient of reaction k depends on the temperature of the particle in accordance with the Arrhenius equation

$$k_k = A_k e^{\frac{-E_k}{RT_p}}, \tag{34}$$

where A_k and E_k are Arrhenius parameters. The pre-exponential factor, A_k, and the activation energy, E_k, are presented in Table 1 for each reaction k in the mechanism.

The distribution of activation energies can be additionally taken info account, then the rate coefficient of reaction k is given by

$$k_k = \int_0^\infty k_k(E) f(E) dE, \tag{35}$$

where $f(E)$ is the activation energy distribution, given by

$$f(E) = \frac{1}{\sigma\sqrt{2\pi}} \exp\left[-\frac{1}{2}\left(\frac{E - E_k}{\sigma}\right)^2\right]. \tag{36}$$

In the equation above, σ is the standard deviation, which can be found in Table 1 for each reaction k.

2.5. Internal particle burning and the effectiveness factor

The rate of reaction k is expressed by Eq. (32). This equation is valid when the concentration of reactants of reaction k inside the particle is uniform. In a situation where the mass transport rates are slower than the chemical reaction rates, the gas does not penetrate the particle completely. As a result, the concentration of reactants inside the particle is not uniform and the rate of reaction k is lower than what is found from Eq. (32). The reduced rate of reaction k can be written as

$$R_{reac,k} = \eta_k k_k \prod_{i=1}^{N_{s,gas}+N_{s,ads}} C_i^{\nu_{i,k}}, \tag{37}$$

where η_k is the effectiveness factor of reaction k. The effectiveness factor is equal to the effectiveness factor of the gas phase reactant in the reaction, which is defined as

$$\eta_i = \frac{R_{spec,i}}{R_{spec,i,max}}, \tag{38}$$

where $R_{spec,i}$ is the actual overall reaction rate of reactant species i and $R_{spec,i,max}$ is the maximum possible reaction rate of reactant species i.

The effectiveness factor is related to the Thiele modulus, ϕ_i, which is a parameter depending on chemistry and mass transport inside the particle.

In some cases, the effectiveness factor is equal to one, i.e. when there is no gas phase reactant in reaction k or the reactant species are net products.

2.6. Mode of char particle conversion

In this paper, the char conversion regimes have been discussed. When the gasification of the char is proceeding in the zone II conversion regime, both the apparent density and radius are reduced during conversion. It is described in the work of Haugen *et al.* [8], that the particle radius starts to decrease when the apparent density at the external surface of the particle goes to zero. This occurs after a certain time of conversion, τ_c, which is defined as

$$\rho_{c,0} = \int_0^{\tau_c} R(r_p, t)dt, \tag{39}$$

where $\rho_{c,0}$ is the initial apparent density of the carbonaceous part of the particle and $R(r_p, t)$ is the overall rate of char conversion at the external surface of the particle. The rate of particle size and apparent density change during char gasification can be written as

$$if \;\; t \leq \tau_c : \qquad \frac{dr_p}{dt} = 0 \quad and \quad \frac{d\rho_p}{dt} = \frac{dm_c}{dt}\frac{1}{V_p}, \tag{40}$$

$$if \;\; t > \tau_c : \qquad \frac{dr_p}{dt} = \frac{dm_c}{dt}\frac{1-\eta}{4\pi r_p^2 \rho_p} \quad and \quad \frac{d\rho_p}{dt} = \frac{dm_c}{dt}\frac{\eta}{V_p}, \tag{41}$$

where the mean effectiveness factor is given by

$$\eta = \frac{R_{reac}}{R_{reac,max}}, \tag{42}$$

where R_{reac} and $R_{reac,max}$ are the sums of molar production rates due to all reactions for all reactants of the global set of reactions for nonuniform and uniform reactant concentration, respectively.

It can be noted that when the time of conversion t is shorter or equal to the time τ_c, the particle size does not change and the apparent density varies proportionally with the mass loss rate. When the time of conversion t is longer than the time τ_c, both particle size and apparent density change due to the mass loss.

3. Results

In this paper simulations of coal char particles exposed to the conditions shown in Table 2 are presented. Conditions presented in Table 2 and the heterogeneous reaction mechanism given in Table 1 describe the base case simulation (Case A).

Table 2: Properties for the simulation.

Property	Value	Unit
Carbon to gas mole ratio	0.35	-
Initial temperature	1400	K
Reactor walls temperature	700	K
Pressure	2.4×10^6	Pa
Initial particle radius	5.0×10^{-5}	m
Particle number density	2.1×10^{10}	m^{-3}
Initial particle density	1300	kg/m^3
Fluid density	5.05	kg/m^3
Initial mole fraction of H_2O	0.50	-
Initial mole fraction of O_2	0.27	-
Initial mole fraction of N_2	0.23	-

The focus is on the effect of H_2, which comes in through the two reactions, R3b and R7f, in which the hydrogen molecule is one of the reactant.

Reaction R3b:

$$H_2 + 2C_f \rightarrow C(H) + C(H) \tag{43}$$

where two free carbon sites on the particle surface and a hydrogen molecule reacting together become two adjacent carbon sites each having an adsorbed hydrogen atom.

Reaction R7f:

$$C_b + C_f + C(H) + H_2 \rightarrow CH_3 + 2C_f \tag{44}$$

where the free carbon site adsorbs the hydrogen molecule from the gas phase. During the process of reaction, the hydrogen molecule moves, binds to the hydrogen atom adsorbed on the carbon site $C(H)$ and desorbs and leaves the particle as CH_3. An underlying bulk carbon becomes a free carbon site.

In order to check the impact of the hydrogen on char gasification, reactions R3 reverse and R7 forward are simulated to be active or not active. Deactivating a reaction means turning it off by temporarily setting its pre-exponential factors

to zero. All other conditions are kept unchanged. In case A, both reactions R3b and R7f are active. In case B, reaction R3b is not active while reaction R7f is active. Case C represents the situation with active reaction R3b and deactivated reaction R7f. In case D, both reactions are turned off. All cases are presented in Table 3. The purpose of this paper is to investigate the impact of H_2 in the gas phase on the time that is needed to reach full conversion of the char particle, and to understand the reasons of this impact. It is assumed that full conversion of a particle is reached when over 99% of the carbon has been consumed.

Table 3: Studied cases A, B, C and D. Reactions R3b, $H_2 + 2C_f \rightarrow C(H) + C(H)$, and reaction R7f, $C_b + C_f + C(H) + H_2 \rightarrow CH_3 + 2C_f$, are simulated to be active or not active.

Case	R3b	R7f
Case A	ON	ON
Case B	OFF	ON
Case C	ON	OFF
Case D	OFF	OFF

It can be seen in the figures below that the results of the simulations are very similar for cases A and C as well as for cases B and D. Similarity for cases A and C means that turning off reaction R7f does not have much influence on the process of conversion. As soon as reaction R3b is deactivated (case B or case D) results are different. It can be concluded that reaction R3b has greater impact on the char conversion process than reaction R7f.

It can be noticed that in the presented figures the lines assigned to results for cases A (black line) and C (yellow line), just as lines assigned to results for cases B (red line) and D (blue line) are exactly on top of each other.

The conversion of the char as a function of time is shown in Fig. 2. It can be seen that cases A and C take much longer to reach full conversion of the char than cases B and D. It can be deduced that deactivating reaction R3b has a strong impact on the conversion rate of the char. In order to understand the reason behind this, the whole chemical reaction process should be investigated. Turning off reaction R3b, that is reducing the pre-exponential factor to zero ($A_{R3b} = 0$), causes a variations in rate of other reactions, what can be seen in Fig. 3. In this figure the molar rate of the most important reactions are compared between cases A and B. The molar rate of reaction k is calculated as the difference between the molar rate of reaction k_f and the molar rate of reaction k_b, where f and b symbolize reaction forward and backward, respectively,

$$R_{reac,k} = R_{reac,kf} - R_{reac,kb}. \tag{45}$$

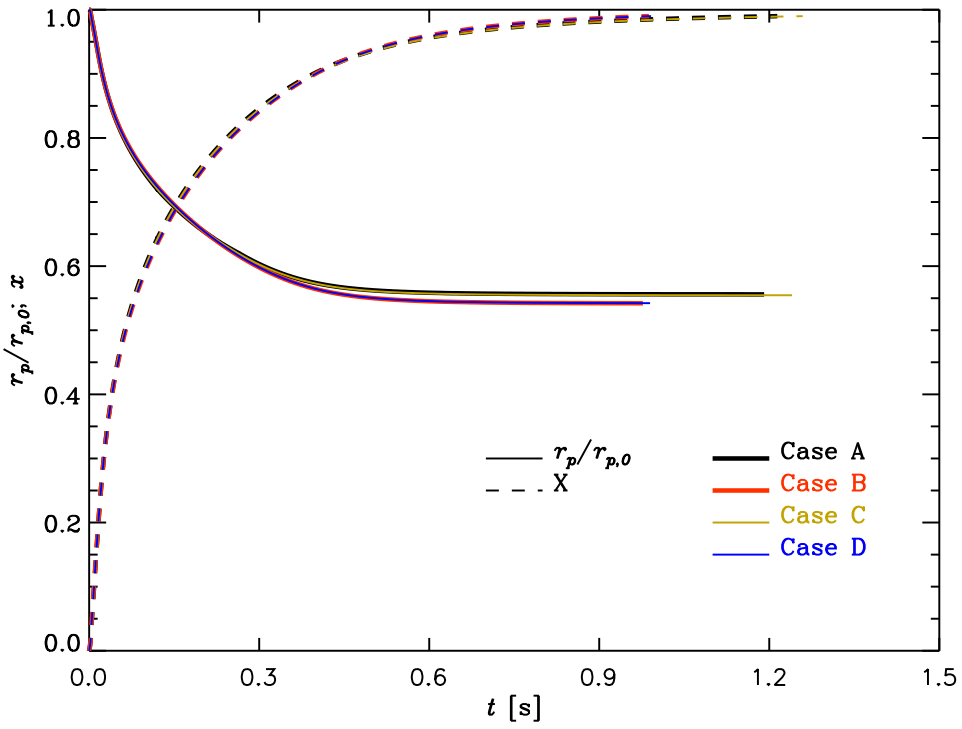

Figure 2: Radius of particle and conversion as a function of time.

It can be noted that lines in the plots are not smooth. There are unexpected peaks for cases A and C for t=0.12 s and t=0.31 s. It may be noticed that these two points could be simply linked by line following predicted path. It is not known exactly the reason why the peaks occur but it seems to not have any consequential effect on the general results.

An hydrogen atom adsorbed on a carbon site, $C(H)$, is the product of reaction R3b, $C(H)+C(H) \leftrightarrow H_2+2C_f$. Deactivation of reaction R3b causes inhibition of $C(H)$ production. The same species is a reactant in reaction R6f, $C_b+C_f+C(H)+H_2O \leftrightarrow CH_3+C(O)+C_f$ and reaction R8, $C_f+C(H)+CO \rightarrow HCO+2C_f$. As a result of having less $C(H)$, the molar rate of both reactions R6 and R8 is slower in case B than in case A. Likewise, $C(H)$ is a reactant in reaction R1b, $2C_f+H_2O \leftrightarrow C(OH)+C(H)$ and reaction R2b, $C(OH)+C_f \leftrightarrow C(O)+C(H)$. In this case the molar rate of reactions R1 and R2 is faster in case B that in case A, since it is the backward reactions that are inhibited. It can be seen that C(H) is

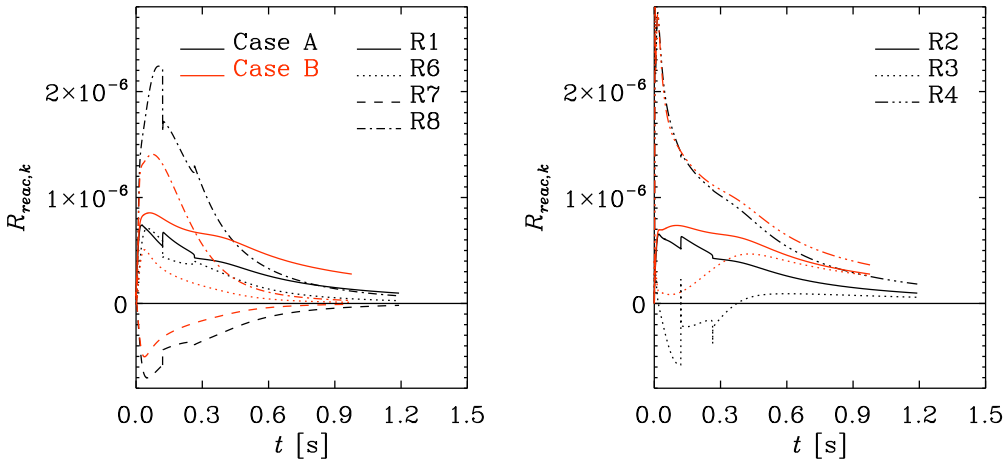

Figure 3: Molar rate of reaction k for cases A and B as a function of time.

also one of the reactants in reaction R7f, $C_b + C_f + C(H) + H_2 \leftrightarrow CH_3 + 2C_f$, but in this case the absolute value of the molar rate of reaction R7 is smaller in case B than in case A. The reason for this is the low concentration of species CH_3, which is limited by reaction R6, which is slower in case B. The molar rate of reaction R4, $C(O) + C_b \rightarrow CO + C_f$, is limited by concentration of $C(O)$. This species is produced in reaction R2f and R6f. Comparing case A and case B, as a result of $R_{reac,R2}$ being faster in case B, $C(O)$ production is intensified and as a result of $R_{reac,R6}$ being slower in case B, $C(O)$ production is reduced. It can be seen in Fig. 3 that the difference of rate of reaction R6 between case A and case B (let it be called difference 6) during the first 0.12 seconds of char conversion is bigger than the difference of rate of reaction R2 between cases A and B (difference 2). That results in lower $C(O)$ concentration and hence a slower rate of reaction R4 in case B. The difference 2 increases and the difference 6 decreases during the conversion process. After the time of 0.12 s, the difference 6 is smaller than difference 2. The concentration of $C(O)$ is high enough to intensify reaction R4, $R_{reac,R4}$ is faster in case B than in case A. When reaction R3b is active (case A), $C(H)$ is primarily produced due to reaction R3, then ($t > 0.37$s) $C(H)$ is consumed, since rate of the reaction forward is higher than rate of reaction backward. As a result of the deactivation of reaction R3b, $C(H)$ is just consumed due to reaction R3 for the whole duration of the gasification process.

In the heterogeneous reaction mechanism, presented in Table 3, the important reactions that are predominantly responsible for char conversion can be identified. Through reactions (R4, R5, R6, R7, R9, R11, R14, R16, R17, R18) carbon is taken from the particle surface, becoming gas phase species. The intensity of

these reactions determinate the overall char conversion rate. Reactions R4, R6, R7, and R14 are also important in terms of high molar reaction rate for studied conditions. Comparing cases A and B, the impact of reaction R14 can be omitted, since the difference of reaction rate for cases A and B is negligible. Reactions R6 and R7 counteract each other, in both cases A and B, as can be seen in Fig. 3. Therefore the principal reaction, governing the char conversion process is reaction R4. As mentioned before, in case B, when the concentration of adsorbed species $C(O)$ is high, reaction R4 is very intense and the molar rate is faster than in case A. This is the main reason for the faster conversion of the char particle for case B.

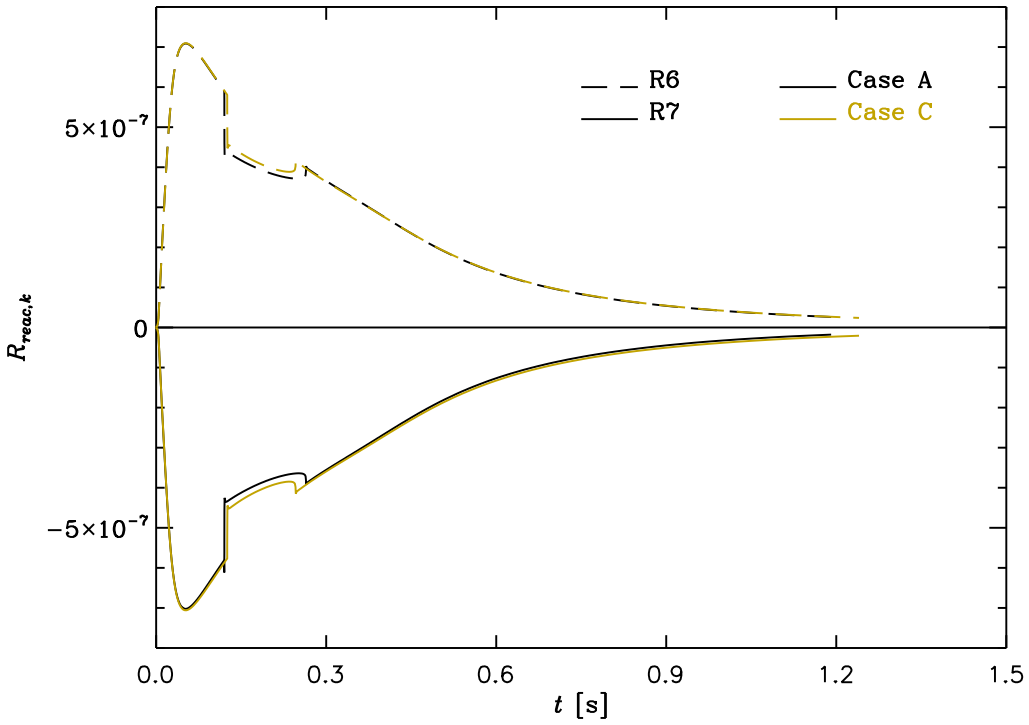

Figure 4: Molar rate of reaction k for cases A and C as a function of time.

It can be noted that, as a result of deactivating reaction R7f, it takes longer to reach full conversion in case C that in case A, as can be seen in Fig. 2. Turning off reaction R7f results in variations of rate of reactions R6 and R7, which is shown in Fig. 4. For reaction R6 the difference of molar rate between cases A and C is almost unnoticeable. For reaction R7 this difference is also very difficult to see in the plot. However, it should be noticed that in Fig. 4, the overall difference, for both reaction forward and backward, is shown. Reaction R7 is one of the reactions governing particle conversion, as it was mentioned before. Therefore deactivation

R7f should have an effect on the time of char conversion, what has been proved and presented in Fig. 2.

The char conversion proceeds very similarly for case B and case D. However, it can be seen in Fig. 2 that the time to reach full conversion is slightly shorter in case B than in case D. This is the result of the combined effects of deactivation of reactions R3b and R6f, as described before.

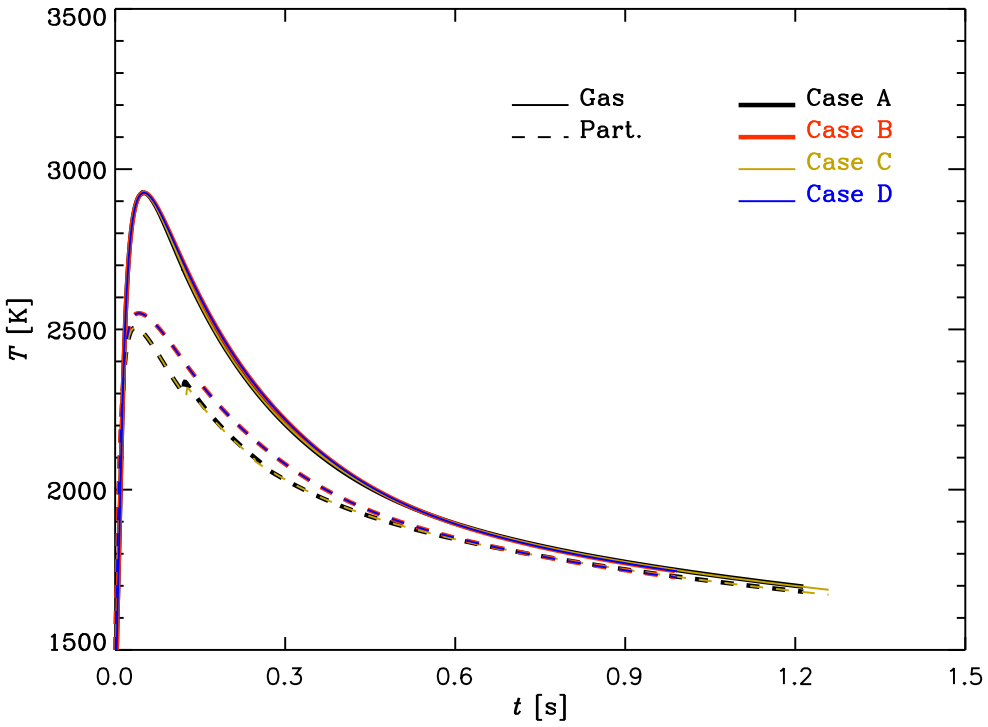

Figure 5: Particle and gas phase temperatures as a function of time.

In Fig. 5 particle and gas phase temperatures as a function of time are shown. It can be seen that at the beginning, both particle and gas phase temperature increase. This is the result of oxidation, which is an exothermic process. In Fig. 7 it can be observed, that it takes less time to consume all the oxygen near the particle surface than far from the particle. Likewise, it can be noted that the peak particle temperature is reached before the gas phase temperature attains maximum value. As soon as the oxygen has been consumed carbon dioxide and steam start to dominate the conversion mechanism. These endothermic reactions cause the particle temperature decrease. As a result of cooling from the particle, the gas phase temperature also decrease.

It can be noticed that the gas phase temperature is very similar for all cases.

The peak particle temperature for cases A and C are lower that for cases B and D. This is due to the greater intensity of endothermic reactions in cases A and C. In Fig. 6 the heating via heterogeneous reactions as a function of time is shown. At the beginning of the char conversion process heat is produced (as an effect of oxidation), later the heat is consumed. It can be seen that the lines symbolizing heating for cases A and C are lower, which means that more heat has to be delivered to proceed the gasification in this cases.

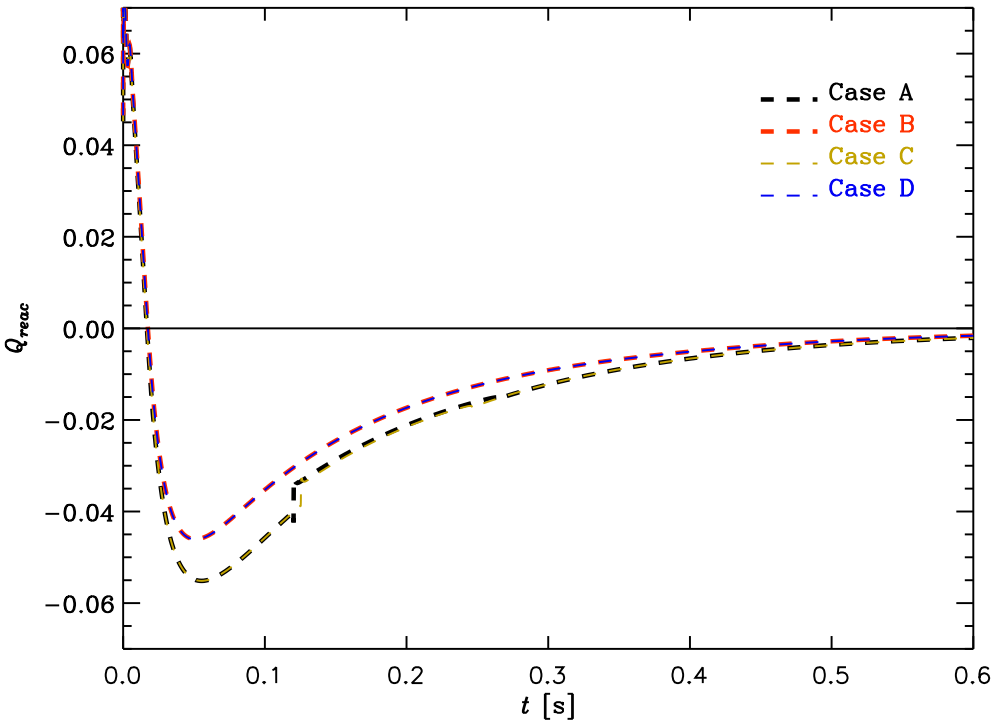

Figure 6: Heating due to heterogeneous reactions as a function of time.

In Fig. 2, the radius of the particle as a function of time is shown. As conversion proceed the size of the particles decrease. It can be seen that at the time when full conversion is reached, the particle radius is smaller for cases B and D than for cases A and C. This is connected with the particle temperature, which is higher for cases B and D. For higher temperatures, the chemical reaction rates are faster, which means that the chemical reactions are more intense at the particle periphery. As an effect, the particle size decreases faster than the particle density.

The mass fraction of the gas phase species as a function of time is shown in Fig. 7. The very first moment of the conversion process can be called combustion, since oxygen reacting with carbon results in heat generation. During combustion,

O_2 is consumed and CO_2 is produced very quickly. After the oxygen has been consumed, gasification of char by CO_2 and H_2O starts to dominate the process. This explains the decreasing amounts of carbon dioxide and hydrogen in the gas phase. The amount of CO and H_2 in the gas phase increase, as an effect of char gasification.

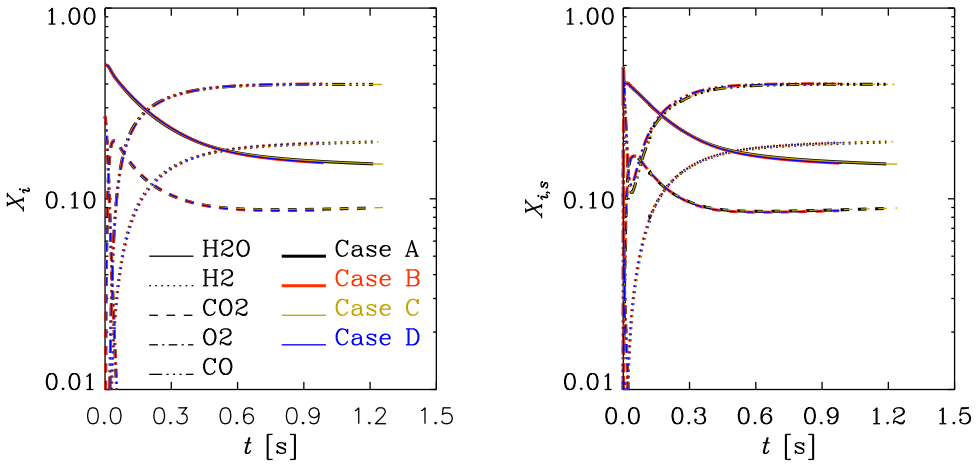

Figure 7: Gas phase species (left panel) and mole fraction of gas phase near to the surface of particle (right panel) as a function of time.

In Fig. 7, the mole fraction of the gas phase near the surface of the particle as a function of time can be seen. Combustion takes place mainly at the particle surface, where the amount of O_2 decreases faster than at some distance from the particle. First, the amount of CO increase very fast as a result of incomplete combustion, then, it quickly decrease while being oxidized to CO_2. As soon as gasification with steam and carbon dioxide starts, both these mass fractions decrease and the fraction of carbon monoxide and hydrogen increase.

The amount of species either near or away from the particle surface is the same for all cases. It can be inferred that deactivation of reaction R3b, R7f or both does not influence the fraction of species i in the gas phase. The gas phase reach the chemical equilibrium.

In Fig. 8, the surface fraction of adsorbed species as a function of time is shown. It can be noted that the fraction of free carbon sites during the whole conversion process is close to unity. That may suggest that the rate of conversion is limited by particle adsorption ability. In the plot, the differences between adsorbed species fraction of $C(O)$, $C(OH)$ and $C(H)$ for each case can be seen. The amount of oxygen adsorbed on the carbon site is initially lower in case B and D than in case A and C. The fraction of $C(O)$ for cases B and D increases faster than

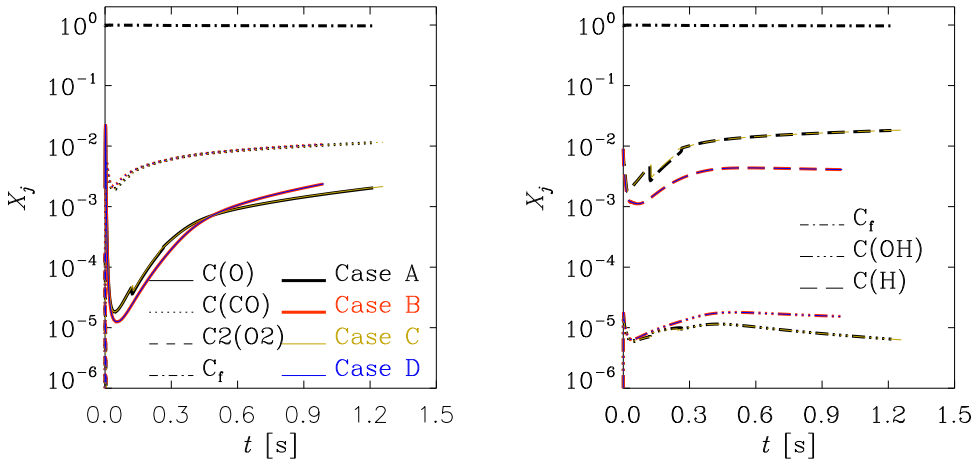

Figure 8: Surface fraction of adsorbed species as a function of time.

for cases A and C during conversion process and after $t = 0.5$ s it is higher. This results from changed molar rate of reactions R2 and R6. Due to these reactions $C(O)$ is produced, what has been described before. The amount of hydrogen adsorbed on the carbon side is lower in case B and D than in case A and C. It is clear, that this effect is caused by deactivation of reaction R3b, the main reactions which due to $C(H)$ is produced. The amount of $C(OH)$ is higher in case B and D than in case A and C. The reason for this is more intensive production of $C(OH)$ due do reaction R1 having higher molar rate in cases B and D.

3.1. Impact of the temperature inside the reactor

In this section the impact of the hydrogen in the gas phase on char gasification at low, intermediate and high temperatures is studied. It is assumed that the temperature inside the reactor during the conversion process is constant.

Table 4: Properties for the simulation at constant temperature inside the reactor.

Property	Value	Unit
Carbon to gas mole ratio	0.5	-
Reactor wall temperature	700	K
Pressure	2.4×10^6	Pa
Initial particle radius	5.0×10^{-5}	m
Initial particle density	1300	kg/m^3
Initial mole fraction of H_2O	0.50	-
Initial mole fraction of O_2	0.45	-
Initial mole fraction of N_2	0.05	-

Conversion of the char particle exposed to the conditions shown in Table 4 and reacting according to the set of reactions presented in Table 1, describe the base case simulation (Case A). See Table 3 for a description of the other cases (B, C and D).

In this section the conversion of the char at different temperatures has been studied. It is assumed that the initial temperature (which is the same for the gas phase and particle) does not change during the gasification process. It has been found, that in the conditions described in Table 4, the full conversion of the particle (i.e. when $x > 0{,}99$) can be reached in the temperature range 1150 K to 2650 K.

The time to reach full conversion as a function of temperature is shown in Fig. 9. The time to reach full conversion is symbolized by τ. It can be noted, that the lower temperature, the longer time is needed to reach full conversion. At high temperatures ($T > 1900K$), the full conversion takes less than 1 s. It can be also seen, that in the temperature range 1150 K to 2000 K the full conversion is reached faster for cases B and D than for cases A and C. At very low temperature ($T < 1400K$), it can be observed that τ is longer for case C than for case A. In the temperature range 2000 K to 2650 K, it takes longer to reach full conversion for cases B and D than for cases A and C. It can be concluded that the temperature of gasification affects the time it takes for the char to reach full conversion. The impact of the hydrogen on the char gasification strongly depends also on the temperature inside the gasifier.

It is the purpose of this paper to compare the time it takes for the char to reach

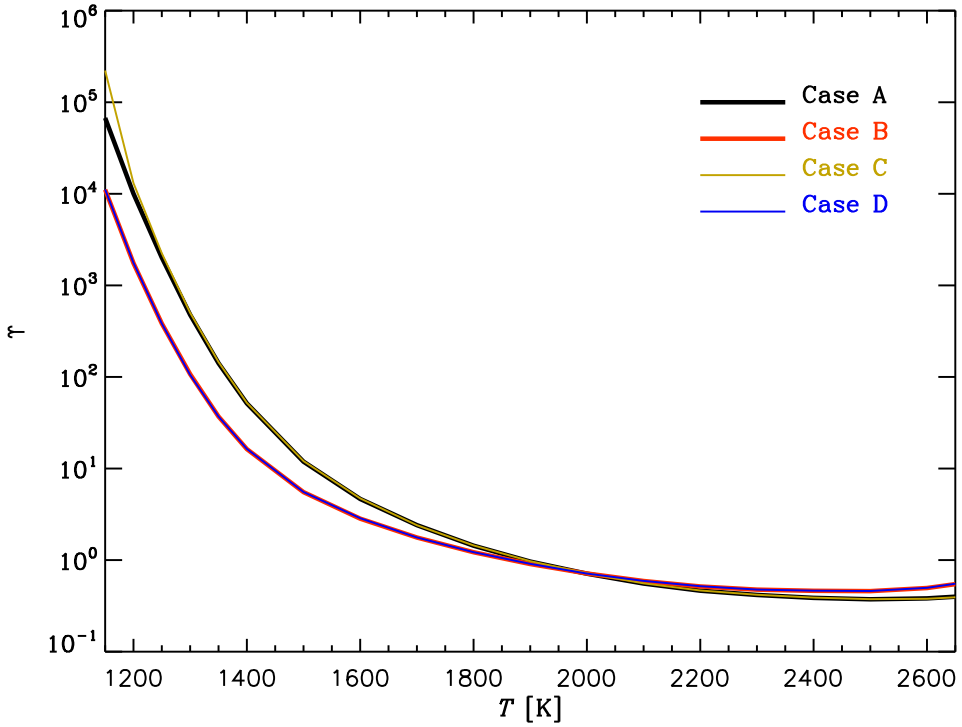

Figure 9: Time to reach full conversion of the char as a function of temperature.

full conversion in each case, where one of the hydrogen reactions (cases B and C) or both of them (case D) are deactivated, with the time it takes to reach full conversion in base case (case A), in the different conditions of the temperature. This relationship can be expressed by the ratio of the time to reach full conversion in cases B, C and D, respectively, to the time to reach full conversion in case A. The ratio is symbolized by α and can be written as

$$\alpha_B = \frac{\tau_B}{\tau_A}, \tag{46}$$

$$\alpha_C = \frac{\tau_C}{\tau_A}, \tag{47}$$

$$\alpha_D = \frac{\tau_D}{\tau_A}, \tag{48}$$

where τ_A, τ_B, τ_C and τ_D represent the time to reach full conversion in case A, B, C and D, respectively.

In Fig. 10, the relative time to reach full conversion of the char as a function of temperature for cases with (black line) and without (colored lines) hydrogen

reactions is shown. It can be seen that α_B and α_D increase with the increasing temperature, reach unity at temperature about 2000 K and continue to increase. It can be also seen that α_C decrease with the increasing temperature, reach unity at temperature about 1400 K and remain equal to unity at higher temperatures.

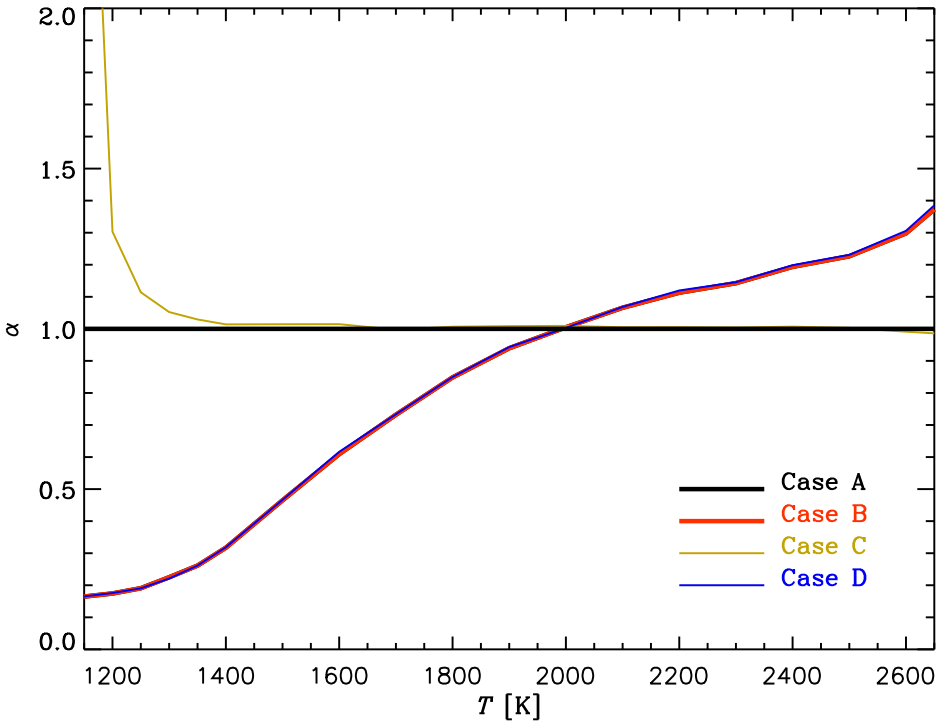

Figure 10: Relative time to reach full conversion of the char as a function of temperature.

Summarizing, the deactivation of the hydrogen containing reactions has an impact on the time to reach full conversion of the char in the entire temperature range. At low and intermediate temperatures hydrogen inhibits, and at high temperatures, it speeds up gasification. Analyzing the individual reactions, turning off reaction R3b results in the faster conversion at low temperatures, and at high temperatures it causes the slower conversion. The deactivation of the reaction R7f has an impact on the time of full conversion just at very low temperatures, τ_C is longer in this case.

In order to study the mechanism behind the impact of the hydrogen on the char gasification, the detailed chemical reaction process has been investigated for three selected temperatures: the lowest and the highest temperature, which for the full conversion of the char still can be reached, 1150 K and 2650 K, respectively, and

the temperature of 2000 K, where the time to reach full conversion is almost the same in all cases.

The mechanism employed in this work is designed to study the process of gasification at low and intermediate temperatures. However, in this section, the mechanism has been used to simulate the char gasification in a much wider temperature range. It can be seen from the figures presenting results of the conversion of the char at very high temperature of 2650 K that an atypical peak occurs. It can be deduced that the mechanism does not work correctly in these conditions. However, the mentioned anomaly seems to not have any substantial impact on the overall results of the research.

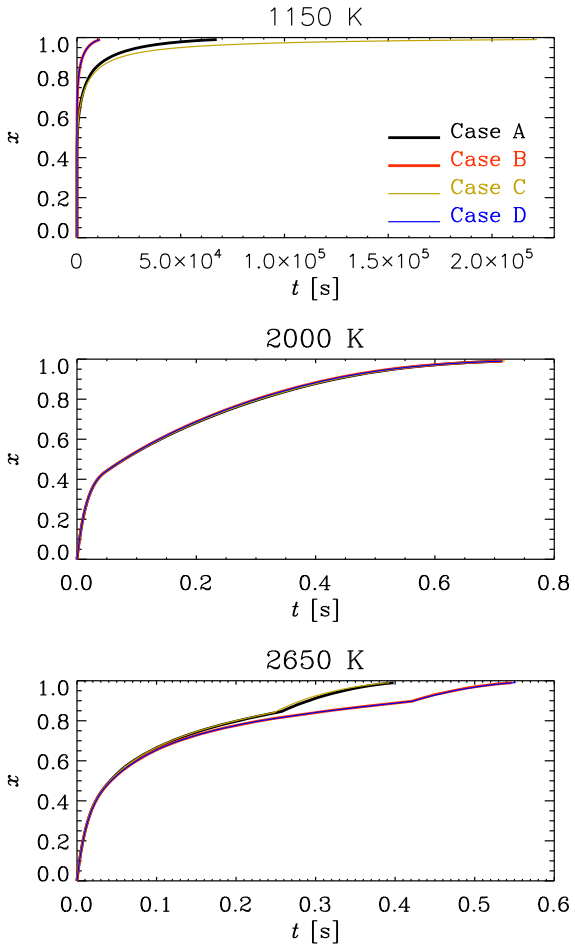

Figure 11: Conversion as a function of time at temperature of 1150 K, 2000 K and 2650 K.

In Fig. 11, the conversion as a function of time for the different temperatures

is shown. At temperature of 1150 K the time to reach full conversion is very long. In cases B and D it is shorter, and in case C it is longer than in base case (case A). At temperature of 2000 K the conversion is faster than at temperature of 1150 K. The time to reach full conversion is the same for all cases. At temperature of 2650 K reaching full conversion takes the shortest time, and it is reached faster for cases A and C than for cases B and D.

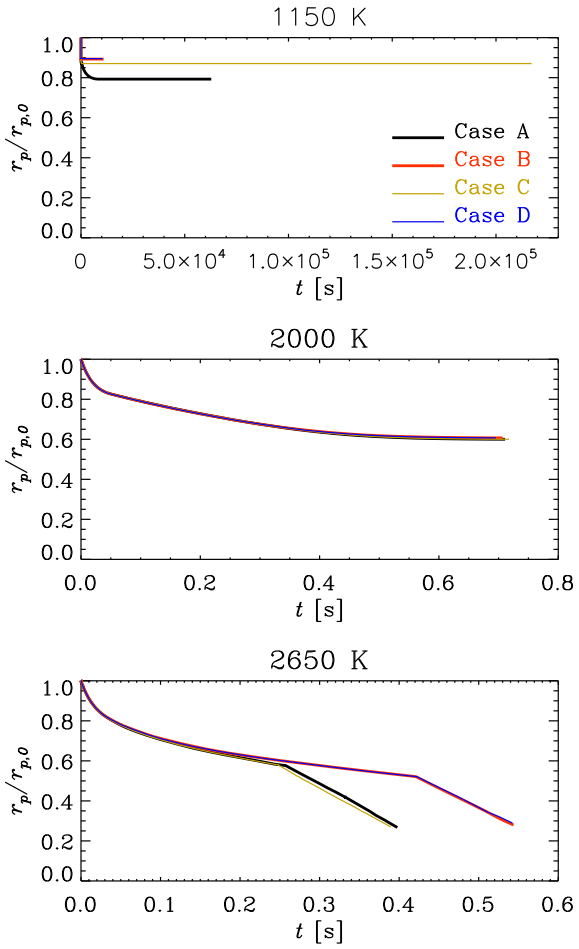

Figure 12: Particle radius as a function of time at temperature of 1150 K, 2000 K and 2650 K.

In Fig. 12, the radius of the particle as a function of time in different conditions of temperature is shown. It can be seen that, as the temperature is higher, the size of the particle is smaller at the end of the conversion process. The reason for this are chemical reaction rates, which are faster at high temperatures. In result, the gasification takes part mainly at the particle periphery, so the radius of

the particle decreases faster than the particle density. At temperature of 1150 K, the particle radius decreases at the beginning of the conversion process, then it remains constant. It can be noted that the size of the particle is smaller in case A than in cases B, C and D. This means that for cases with deactivated hydrogen containing reactions, the effectiveness factor is closer to unity than for case, where the full reaction mechanism is used. It can be concluded that turning off hydrogen reactions causes more uniform concentration of the reactive gas inside the particle. At temperature of 2000 K, the rate of change of the radius is the same for all cases. At temperature of 2650 K, the size of the particle change faster for cases A and C than for cases B and D, but at the end of the conversion process it is the same for all cases, the particle radius is very small. This is the result of the fast chemical reaction rates at very high temperature inside the reactor. Almost all conversion proceeds at the particle periphery.

In order to understand the differentiated impact of the hydrogen on the char gasification, depending on the temperature inside the gasifier, the whole chemical reaction process has been investigated for each temperature: 1150 K, 2000 K and 2650 K.

At temperature of 1150 K, the deactivation of reaction R3b results in the change of the molar rate of other reactions (R1, R2, R4, R10 and R11). An hydrogen atom adsorbed on a carbon site, $C(H)$, is produced due to reaction R3b. Turning of this reaction causes inhibition of $C(H)$ production. The same species is a reactant in reaction R1b, $2C_f + H_2O \leftrightarrow C(OH) + C(H)$ and reaction R2b, $C(OH) + C_f \leftrightarrow C(O) + C(H)$. As a result of having less $C(H)$, the molar rate of both reactions R1 and R2 is faster, since it is the backward reactions that are inhibited. The molar rate of reactions R4, $C(O) + C_b \rightarrow CO + C_f$, R10b, $CO_2 + C_f \leftrightarrow C(O) + CO$ and R11 $C_b + CO_2 + C(O) \rightarrow 2CO + C_f$ is limited by concentration of $C(O)$, which is higher in case B than in case A, because of the lower consumption due to reaction R2b. The reactions R4, R10b and R11 are intensified, which determines the faster overall char conversion rate, since through reactions R4 and R11 carbon is taken from the particle surface, becoming gas phase species.

At temperature of 1150 K, the deactivation of reaction R7f results in the change of the molar rate of other reactions (R1, R2, R4, R6, R7 and R8). Since an hydrogen atom adsorbed on a carbon site, $C(H)$, is one of the reactant of reaction R7f, turning off this reaction, results in the lower consumption of $C(H)$. The concentration of $C(H)$ is higher, which intensifies reactions R1b, $2C_f + H_2O \leftrightarrow C(OH) + C(H)$, R2b, $C(OH) + C_f \leftrightarrow C(O) + C(H)$, R6f, $C_b + C_f + C(H) + H_2O \leftrightarrow CH_3 + C(O) + C_f$ and R8, $C_f + C(H) + CO \rightarrow HCO + 2C_f$, in which $C(H)$ is one of the reactants. The intensification of reaction R2b causes the higher consumption of $C(O)$. In result, the molar rate of reactions R4, $C(O) + C_b \rightarrow CO + C_f$ is lower, since there is not enough adsorbed oxygen to run the reaction. In case

C, the molar rate of two principal reactions governing the conversion process, R4 and R7, is reduced, which results in the slower overall char conversion rate.

In case with deactivated both reaction, R3b and R7b, the effect is exactly the same as in case with deactivated just reaction R3b, which is likely much more important than reaction R7f.

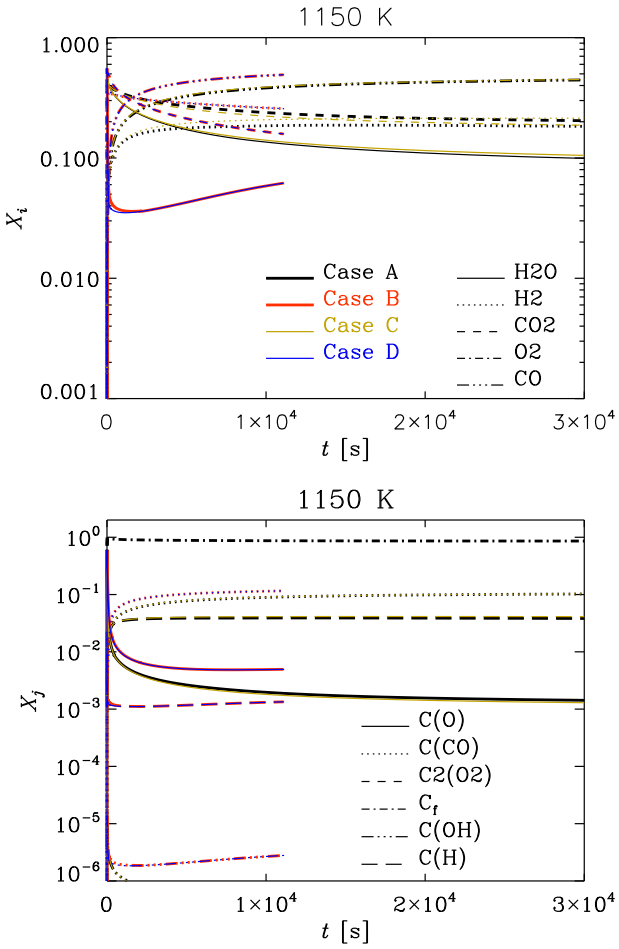

Figure 13: Gas phase species (top panel) and surface fraction of adsorbed species (bottom panel) as a function of time at temperature of 1150 K.

In Fig. 13, the gas phase species as a function of time at temperature of 1150 K is shown in the top panel. It can be seen that the amount of hydrogen is higher in cases B and D than in cases A and C, since it is not consumed due to reaction R3b, which is deactivated. The mass fraction of H_2O is limited by reaction R2. The slower reaction R2b hence the lesser production of H_2O, and as a result, the lower concentration in the gas phase for cases B and D than for cases A and C.

The faster reactions R4 and R11 cause the more intensive production of CO, so the amount of this species in the gas phase is higher in cases B and D than in cases A and C. Due to reaction R11, CO_2 is consumed, the mass fraction of this species is lower in cases B and D than in cases A and C. It can be noted that the mass fraction of gas phase species is the same in cases A and C, even if the conversion rate is different for both cases. It can be concluded that in case with deactivated reaction R7f, the chemical equilibrium of the gas phase is reached. Similarly, in Fig. 13, just the difference between surface fraction of adsorbed species between cases A and B can be noted. In this situation, two of the most important species are oxygen and hydrogen adsorbed on the carbon site. The amount of $C(H)$ in cases B and D is lower than in cases A and C, since it is not produced due to reaction R3b. The concentration of $C(O)$ is higher in cases B and D. The reason for this is the lower consumption via reaction R2b.

In Fig. 14, the species production rate due to the gas-to-particle reactions as a function of time is shown. The difference between the gas phase species fraction for cases A and B can be seen in the Fig. 13, although the rate of the species production is the same. It should be taken into consideration, that there is also species production due to gas-to-gas reactions. In Fig. 14, the positive values of the rate represent the overall production of the species and negative values represent the overall consumption of species i. It can be noted that during the first step of gasification, the combustion, the carbon is oxidized and both carbon dioxide and carbon monoxide are produced. It can be also noted that as a result of steam consumption, hydrogen is produced. As the time of the gasification process is longer, the species production rate is closer to zero, what means that most of the reactions between the gas and the char particle take part at the beginning of the process. Later the reaction rates are very slow, what is the reason of very long conversion of the char.

The deactivation of reaction R3b, at temperature of 2000 K, does not influence the rate of the conversion, however it does have an impact on the rate of other reactions (R1, R2, R4, R6, R7, R8, R13). As a result of lower concentration of $C(H)$, reactions R1b, R2b, R6f and R8f slow down. Since CH_3 is less produced due to reaction R6f, reaction R7b, $C_b + C_f + C(H) + H_2 \leftrightarrow CH_3 + 2C_f$, also slows down. The rate of reaction R4 depends on the concentration of $C(O)$, which is one of the reactant of reaction R2b and one of the product of reaction R6f. Firstly, the difference of molar rate of reaction R2 between cases A and B is bigger then the difference of molar rate of reaction R6 between cases A and B, after this difference is smaller. As a result, at the beginning of the process, reaction R4, which is directly responsible for the conversion is faster in B than in case A, then it is slower. Additionally, due to reduced consumption of CO in reaction R8, with much lower rate in case B than in case A, reaction R13, $CO+C(CO) \rightarrow CO_2+2C_f$, speeds up. This reaction causes putting the carbon atom on the particle surface,

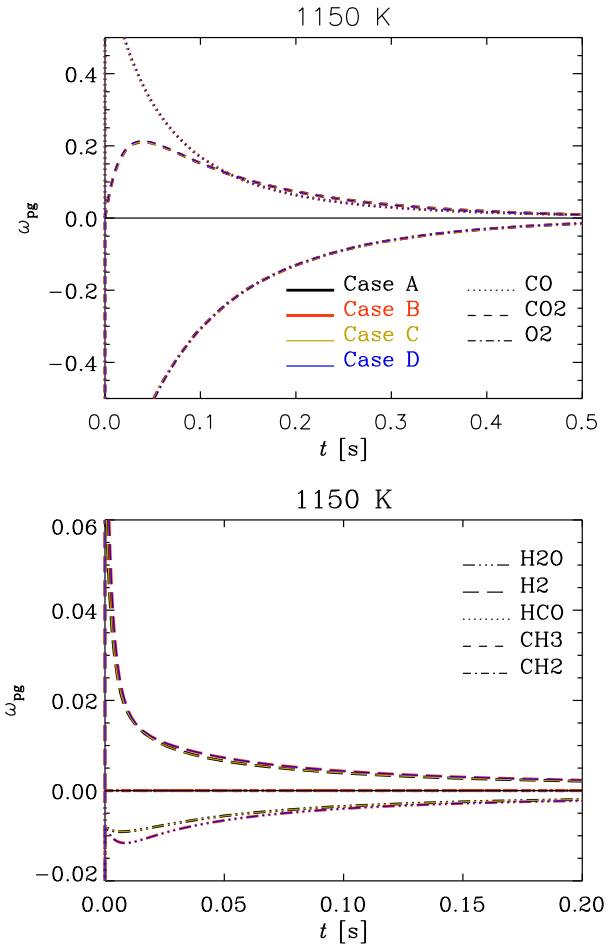

Figure 14: Species production rate due to the gas-to-particle reactions as a function of time at temperature of 1150 K.

what slows down the conversion process. Summing up, the time to reach full conversion is the same for all cases.

The deactivation of reaction R7f, does not influence the molar rates of other reactions. The effect of turning off both reactions, R3b and R7f, is exactly the same for cases B and D.

In Fig. 15, the gas phase species as a function of time at temperature of 2000 K is shown. The gas phase reach the chemical equilibrium, what can be concluded, since the difference between the fractions of each species can not be seen. In the same figure, the surface fraction of adsorbed species in shown. The important difference is between cases A and B for concentration of the hydrogen adsorbed on the particle surface, which is higher in case A, since $C(H)$ is not produced due

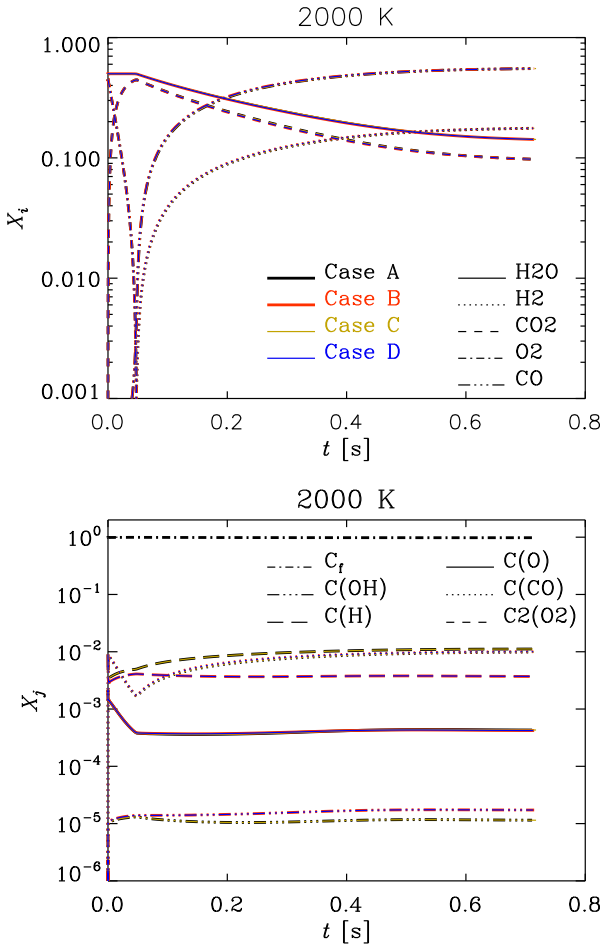

Figure 15: Gas phase species (top panel) and surface fraction of adsorbed species (bottom panel) as a function of time at temperature of 2000 K.

to reaction R3b.

In Fig. 16, the species production rate due to the gas-to-particle reactions as a function of time at temperature of 2000 K is shown. It can be seen, that as oxygen is consumed, the carbon monoxide is produced as a result of not complete combustion, first and then, as a result of gasification due to CO_2. It should be also noticed, that the higher overall production can mean the same as the lesser consumption of species. This explains the higher production rate of species CO in case B than in case A. Carbon monoxide is less used in reaction R8, which is slower in case B. Faster reaction R8 is also the reason for the higher production of HCO in base case than in case B. As the gasification due to H_2O proceed, H_2 is produced. As described before, in this situation, the higher overall production

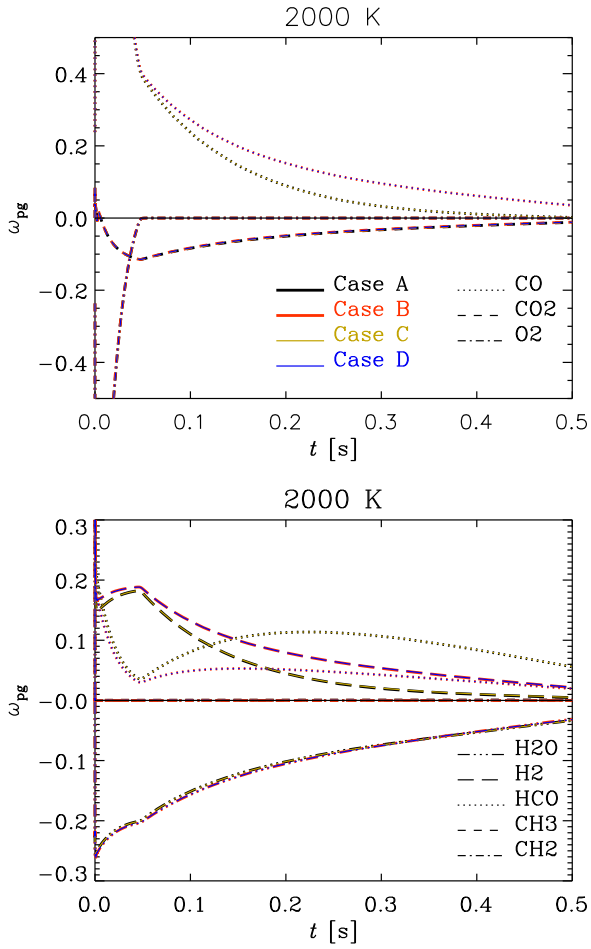

Figure 16: Species production rate due to the gas-to-particle reactions as a function of time at temperature of 2000 K.

of hydrogen in case B than in case A means actually reduced consumption of H_2, what is an effect of deactivation of reaction R3b. The production rate of the species due to the gas-to-particle reactions is the same for cases A and C, as well as for cases B and D.

At temperature of 2650 K, the deactivation of reaction R3b inhibits the conversion of the char by changing the molar rate of other reactions (R1, R2, R4, R6, R7, R8). Turning off reaction R3b results in the lower production of species $C(H)$, the reactant of reactions R1b, R2b, R6f, R8f. The reactions are less intensive in this case. Reaction R7f is also slower, since the fraction of CH_3 is lower. At very high temperatures, the molar rate of reaction R6 is influenced much more than the rate of reaction R2. As a result of very small production of $C(O)$ due to reaction

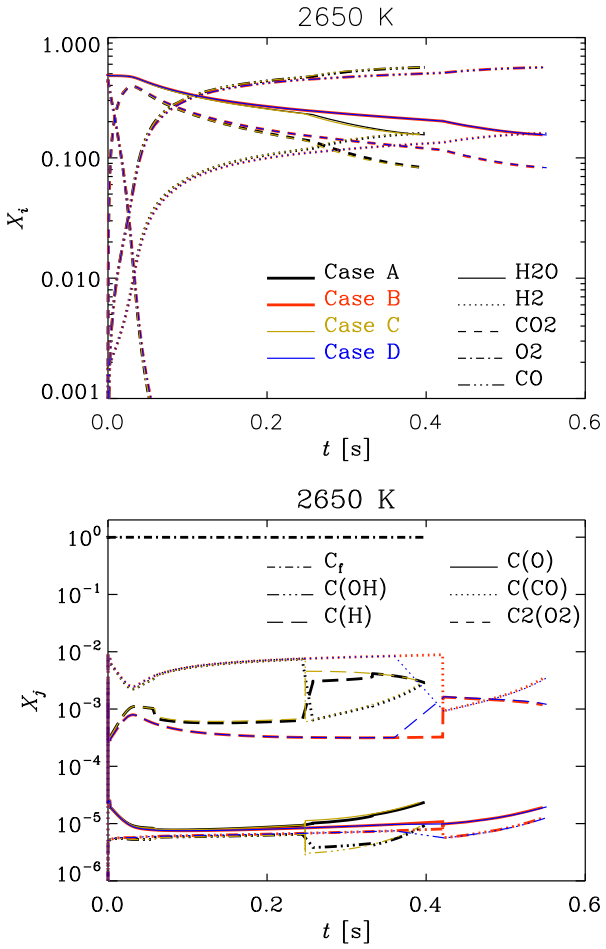

Figure 17: Gas phase species (top panel) and surface fraction of adsorbed species (bottom panel) as a function of time at temperature of 2650 K.

R6f, the rate of reaction R4 is slower in case B than in case A. As mentioned before, reaction R4 is one of the most important in the process of conversion, since a carbon is taken from the particle surface due to this reaction, decorbing as carbon monoxide. Furthermore, the reduced consumption of *CO* due to reaction R8 causes speeding-up reaction R13 in case B. This reaction results in the opposite effect - a carbon is set back at the particle surface, so the conversion slows down. The low molar rate of reaction R4 and the high molar rate of reaction R13 are the main reasons for longer conversion of the char at higher temperatures in the gasifier. The deactivation of reaction R7f has no impact on the rate of char conversion.

In Fig. 17, the gas phase species and the surface fraction of adsorbed species

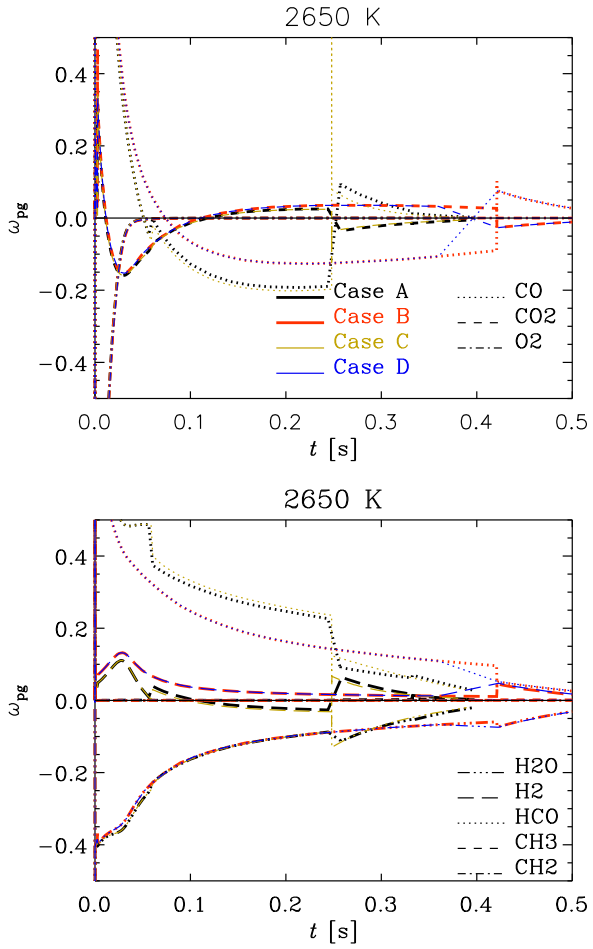

Figure 18: Species production rate due to the gas-to-particle reactions as a function of time at temperature of 2650 K.

as a function of time at temperature of 2650 K is shown. In Fig. 17, it can be seen, that the fraction of gas phase species, as well as the fraction of the species adsorbed on the particle surface is the same for all cases. The only difference is between the surface fraction of $C(H)$ for cases A and B. It is lower in case B, since $C(H)$ is not produced due to reaction R3b.

In Fig. 18, the species production rate due to the gas-to-particle reactions as a function of time is shown for a temperature of 2650 K. As the combustion proceed, oxygen is consumed. At the beginning of the conversion process, carbon dioxide is produced, as a result of the oxidation, then it is consumed, as the gasification due to CO_2 proceed. It can be seen, that after some time, carbon dioxide is overall produced again. The reason for this is the fast rate of reaction R13 in case

B. The rate of production of carbon monoxide decreases with decreasing amount of oxygen in the gas phase to finally reach the negative value, what means the overall consumption of CO. The reason for this is very slow rate of reaction R4 - the slower reaction R4 in case B, the production of CO is lower. Due to gasification, H_2O is consumed and H_2 is produced. It can be seen that the production of H_2 is faster in case B than in case A, since reaction R3b is deactivated. It can be noticed, that the rate of the production of species HCO is higher as the temperature increases. The reason for this is the faster molar rate of reaction R8 at high temperatures. Since in case B, at temperature of 2650 K, reaction R8 is less intensive than in case A, the rate of production of HCO is also slower.

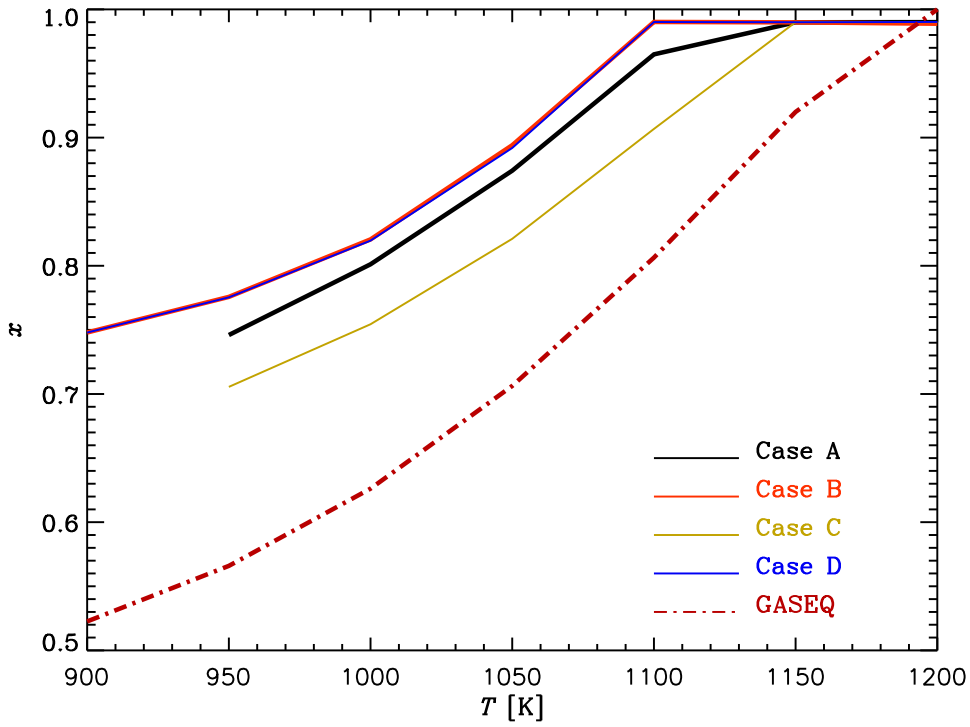

Figure 19: Conversion as a function of temperature.

It can be noted that at very low temperatures the species production rate due to the gas-to-particle reactions is almost the same for all cases, and at higher temperatures it is different for cases with deactivated reaction R3b. The lower temperature inside the reactor, the conversion of the char is longer, so the rate of the production of the species is slower, close to zero. It can be seen in the figures showing the gas phase species and surface fraction of adsorbed species as a function of time, that for conversion at higher temperatures the chemical equilibrium of the gas phase is

reached, since the fractions of the gas species and adsorbed species are the same for all cases. For low temperatures in the gasifier, the opposite, the fractions of the gas species and adsorbed species are different for each case.

In this work, the gasification of char also at low temperatures has been studied. The simulation of the conversion of the char particle at temperatures lower than 1150 K (the lowest temperature for which full conversion is reached for all considered cases) have been performed. The outcomes obtained in this section and the results of simulation in GASEQ [9], a Chemical Equilibrium Program for Windows, have been compared. The simulation of gasification in GASEQ has been performed for the same conditions as assumed in the current section. In Fig. 19 the conversion as a function of temperature at low temperatures is shown. The conversion shown on the y-axis is the conversion of the char when time goes to infinity - i.e. at chemical equilibrium. Hence, these results can be compared to the results from a chemical equilibrium solver (such as GASEQ). It can be seen, that the lower temperature in the gasifier, the lower conversion of the particle is reached at chemical equilibrium. It can be noted that the conversion is going further for cases B and D than for the base case. This confirms the previous conclusions that at low temperatures, the hydrogen inhibits the conversion (for cases B and D). However, in can be also seen, that less carbonaceous material is converted in case C than in case A. Indeed, it has been observed before, that at very low temperatures, the deactivation of reaction R7f causes longer conversion of the char. The results obtained on the basis of GASEQ (dashed line) are similar to the outcomes of the simulations of the model used in this work. Although, it can be noticed that for GASEQ, the conversion is lower for each considered temperature of gasification. The lowest temperature, which for the full conversion of the particle can be reached, is 1200 K. Likely, the slightly different results are due to the fact that the assumptions in employed models are not the same for both cases.

4. Summary

In this work, a newly developed detailed chemical kinetics model for char has been used in order to study the mechanisms behind the hydrogen inhibition and speed-up of char gasification. It is clearly seen that hydrogen inhibition is found for $T < 2000K$, while for $T > 2000K$ the hydrogen in the gas phase speeds up the char conversion. By studying the species reaction rates together with the individual rate of every single reaction, it is shown that hydrogen inhibition at low and intermediate temperatures is due to atomic hydrogen adsorbed on the char surface interacting with atomic oxygen on the surface to form an adsorbed OH molecule. The adsorbed OH molecule combines with another adsorbed hydrogen atom to form gaseous water. The outcome of this is that the adsorbed atomic oxygen, which would normally desorb as gaseous CO while removing a carbon atom from the surface, only takes part in the production of steam, which does not yield any char conversion, and hence the time to reach full conversion is increased due to the presence of hydrogen. It has also been shown that hydrogen speed-up at higher temperatures is due to reaction of adsorbed hydrogen atom with steam and carbon atom producing atomic oxygen adsorbed on the surface. As a result of high concentration of $C(O)$ the process of removing carbon atom from the surface is also faster. Additionally, while hydrogen occurs in the gas phase, the consumption rate of carbon monoxide in reaction with adsorbed atom of hydrogen and carbon atom is intensified. This inhibits the interaction of gaseous carbon monoxide and adsorbed carbon monoxide, which would normally desorb as carbon dioxide while a carbon atom would be set back on the particle surface, so conversion would be longer. The presence of hydrogen in the gas phase for gasification at higher temperatures results in a decrease the time to reach full conversion.

References

[1] Mitchell, R.E., Campbell, P.A. & Ma, L.: 2006, "Characterization of Coal and Biomass Conversion Behaviors in Advanced Energy Systems" , *GCEP Technical Report 2006*

[2] Thiele, E.W.: 1939 "Ing. Eng. Chem.", **31**, 916

[3] Autodesk, AutoCAD

[4] Haugen, N. E. L., Mitchell, R. E. & Tilghman, M. B.: 2015, "A comprehensive model for char particle conversion in environments containing O_2 and CO_2", *Combustion & Flame*, **162**, 1455-1463

[5] Haynes, B. S.: 2001, "A turnover model for carbon reactivity I. development", *Combustion & Flame*, **126**, 1421-1432

[6] Haugen, N. E. L., Kruger, J., Løvås, T., J., Mitchell, R. E. & Tilghman, M. B.: 2014, "Transient simulations of biomass char gasification", *Proceedings of the 1st International Workshop on CFD and Biomass Thermochemical Conversion*

[7] Tilghman, M. B & Mitchell, R. E.: 2015, "Coal and biomass char reactivities is gasification and combustion environments", *Combustion & Flame*

[8] Haugen, N. E. L., Mitchell, R. E. & Tilghman, M. B.: 2014, "The conversion mode of a porous carbon particle during oxidation and gasification", *Combustion & Flame*, **161**, 612

[9] Microsoft Windows, GASEQ